Materials Science-Poland, *Vol. 26*, *No. 3*, *2008*

Electrical properties of $0.90Pb[(Mg,Zn)_{1/3}Ta_{2/3}]O_3$–$0.10PbTiO_3$ relaxor

S. PRASAD[1*], K. PRASAD[1**], S.N. CHOUDHARY[1], T.P. SINHA[2]

[1] Materials Research Laboratory, University Department of Physics, T. M. Bhagalpur University, Bhagalpur 812 007, India

[2] Department of Physics, Bose Institute, 93/1 A.P.C. Road, Kolkata 700 009, India

Polycrystalline $0.90Pb[(Mg_{2/3}Zn_{1/3})_{1/3}Ta_{2/3}]O_3$–$0.10PbTiO_3$ having a tetragonal perovskite type structure was prepared by the high temperature solid-state reaction method. Dielectric studies showed the relaxor behaviour with a diffuse phase transition. A high value of ε_{max} (> 10 000) was achieved with the temperature T_m of maximum permittivity around room temperature at 1 kHz. The frequency dependence of T_m was modelled using the Vogel–Fulcher law. The dielectric relaxation in the material investigated here was found to be analogous to the magnetic relaxation in a spin-glass system. The shape of the complex impedance curve indicated that the system exhibited almost the Debye type dielectric relaxation at 350 °C, where as a non-Debye profile was observed at temperatures below 325 °C. Furthermore, the relaxation frequency was found to shift towards higher frequencies upon increasing temperature.

Key words: *relaxor ferroelectrics; dielectric property; diffuse phase transition; dielectric relaxation*

1. Introduction

Relaxor ferroelectrics such as $Pb(Mg_{1/3}Nb_{2/3})O_3$, $Pb(Zn_{1/3}Nb_{2/3})O_3$, $Pb(Ni_{1/3}Nb_{2/3})O_3$, $Pb(Mg_{1/3}Ta_{2/3})O_3$, $Pb(Sc_{1/2}Ta_{1/2})O_3$, $Pb(Fe_{1/2}Nb_{1/2})O_3$, etc. have been extensively studied for their use in multilayer capacitors (MLCs) and for electrostrictive applications. Among these $Pb(Mg_{1/3}Nb_{2/3})O_3$ (PMN) and its solid solutions with other compounds like $PbTiO_3$, $BaTiO_3$, etc. are the most widely studied. These compounds are generally characterized by their frequency dependent broad maximum in the temperature dependence of dielectric permittivity. However, $Pb(Mg_{1/3}Ta_{2/3})O_3$ and its solid solutions have been given comparatively little attention. As $Pb(Mg_{1/3}Ta_{2/3})O_3$ also exhibits disordered perovskite structure and typical relaxor ferroelectric properties, its preparation in pure or modified form and subsequent characterization deserve further investigation.

---

[*]Permanent address: Department of Physics, B.N. College, Bhagalpur 812 007, India.
[**]Corresponding author, e-mail: k_prasad65@yahoo.co.in; k.prasad65@gmail.com

Lead magnesium tantalate $Pb(Mg_{1/3}Ta_{2/3})O_3$ (PMT) is a well known relaxor ferroelectric having anomalously large electric permittivity and a broad diffuse phase transition [1] near – 98 ºC. On the other hand, lead titanate $PbTiO_3$ (PT) is a normal ferroelectric exhibiting a sharp peak in the electric permittivity and its Curie temperature is around 490 ºC. As PMT has a highly tolerant ABO_3 structure, it provides enough scope for modification either at the *A*- or *B*-site. It has been observed that the electrical properties and the temperature of the maximum of permittivity T_m of PMT can be controlled effectively by proper doping at *B*-site. Also, the addition of PT in PMT offers an advantage to shift the phase transition temperature to the higher temperature side [2, 3].

To the best of our knowledge, even after having made an extensive literature survey, there has been no report so far on the polycrystalline $0.90Pb[(Mg_{2/3}Zn_{1/3})_{1/3}Ta_{2/3}]O_3$ $–0.10PbTiO_3$ (PMZT-PT (90/10)). We recently studied a similar relaxor system, namely $0.80Pb[(Mg_{2/3}Zn_{1/3})_{1/3}Ta_{2/3}]O_3–0.20PbTiO_3$, which showed good dielectric properties. The value of T_m was found to be 57 ºC with ε_{max} = 8412 at 1 kHz [4]. Furthermore, in order to bring T_m near to room temperature, the percentage of added PT was reduced in this work. Accordingly, the present study considers the dielectric response of PMZT-PT(90/10) ceramic prepared through the columbite precursor method over a wide range of frequencies and temperatures. Impedance spectroscopy and Cole –Cole formalism were employed in order to investigate the dielectric relaxation in PMZT-PT(90/10) ceramic. Despite earlier investigations, the mechanism responsible for freezing processes in relaxor ferroelectrics is yet to be completely understood. A similar system, PMN, was earlier found to have analogies with the spin-glass system in which thermally activated polarization fluctuations occurred above a static freezing temperature T_f. Based on this fact, it is considered that the relaxor ferroelectric behaves much like a polar-glassy system, which can be modelled through the Vogel–Fulcher law [5, 6]:

$$f = f_0 \exp\left(-\frac{E_a}{k_B\left(T_m - T_f\right)}\right) \tag{1}$$

where f is the operating frequency, f_0 – the pre-exponential factor, k_B – the Boltzmann constant and E_a is the activation energy. Accordingly, to understand the mechanism responsible for the freezing process in PMZT-PT(90/10), dielectric data were modelled using the Vogel–Fulcher relation in the present investigation.

2. Experimental

$0.90Pb[(Mg_{2/3}Zn_{1/3})_{1/3}Ta_{2/3}]O_3–0.10PbTiO_3$ ceramic was prepared by the standard dry route, using a two-stage process. First, a columbite ($Mg_{2/3}Zn_{1/3}Ta_2O_6$) precursor was prepared at 1000 °C for 5 h using $MgCO_3$, ZnO and Ta_2O_5, according to the thermochemical reaction:

$$\frac{2}{3}\mathrm{MgO}+\frac{1}{3}\mathrm{ZnO}+\mathrm{Ta_2O_5}\xrightarrow{\Delta}\mathrm{Mg_{2/3}Zn_{1/3}Ta_2O_6}$$

This was then recalcined with PbO at 900 °C for 4 h to yield Pb[($Mg_{2/3}Zn_{1/3}$)$_{1/3}$ $Ta_{2/3}$]O_3. The chemical reaction taking place was as follows:

$$\mathrm{PbO}+\frac{1}{3}\mathrm{Mg_{2/3}Zn_{1/3}Ta_2O_6}\xrightarrow{\Delta}\mathrm{Pb[(Mg_{2/3}Zn_{1/3})_{1/3}Ta_{2/3}]O_3}$$

The purity of chemicals used was higher than 99%. Finally, 10 wt. % of PT was mixed with PMZT to obtain the desired compound: 0.90Pb($Mg_{2/3}Zn_{1/3}$)$_{1/3}$$Ta_{2/3}O_3$ –0.10$PbTiO_3$. Further cylindrical pellets of 0.90 mm in diameter and 1.52 mm thick were prepared under an isostatic pressure of 6×10^7 N·m^{-2}. Polyvinyl alcohol was used as a binder. The pellets were then sintered at 1200 °C for 2 h. The formation of the compound was checked by X-ray diffraction (XRD) using an X-ray diffractometer (Phillips PW1710, Holland) with CuK_α radiation λ = 1.5443Å over a wide range of Bragg angles ($20° \le 2\theta \le 80°$). To study the electrical properties, both flat surfaces of the pellets were electroded with a fine silver paint, and subsequently dried at 200 °C for 1 h before conducting the experiment. Electrical impedance Z, phase angle θ, capacitance and the dissipation factor of the sample were measured both as a function of frequency (0.1 kHz–3 MHz) as well as of temperature (20–350 °C) using a computer controlled LCR-Hightester (HIOKI 3532, Japan).

3. Results and discussion

3.1. Structural studies

A standard computer program (POWD) was used for the XRD-profile (Fig. 1) fitting. There was good agreement between the observed and calculated inter-planer

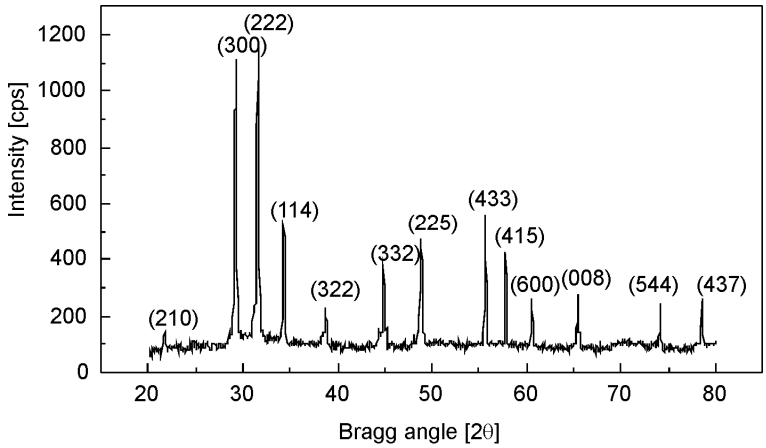

Fig. 1. X-ray diffraction pattern of 0.90Pb[($Mg_{2/3}Zn_{1/3}$)$_{1/3}$$Ta_{2/3}$]$O_3$–0.10$PbTiO_3$ at room temperature

spacing (*d*-values). There was no trace of any extra peaks due to constituent oxides which suggests the compound has a single-phase tetragonal structure. The lattice parameters were found to be: a = 9.159Å and c = 11.412Å, with an estimated error of $\pm 10^{-3}$Å. The criterion adopted for evaluating the correctness, index reliability, and the structure of PMZT-PT was the sum of differences between observed and calculated *d*-values (i.e., $\Sigma \left| d_{\text{obs}} - d_{\text{cal}} \right|$ to be a minimum. The tetragonal axial ratio (c/a) and unit cell volume (a^2c) have been estimated to be 1.246 and 957.32 Å^3, respectively. Hence, decreasing the percentage of PT reduces both the tetragonal axial ratio as well as the unit cell volume [4].

3.2. Dielectric studies

Figure 2 illustrates the temperature dependence of the electric permittivity ε and the dissipation factor tan δ at various frequencies. The plots show a broad maximum (diffuse phase transition, denoted as DPT) around 10 °C, and show strong frequency dispersion which indicates the relaxor behaviour of PMZT-PT. It was observed that the temperature T_m of maximum permittivity shifted to higher temperatures (from 29 ºC at 1 kHz to 35 °C at 1 MHz) while ε_{max} decreased (from 10 426 at 1 kHz to 6923 at 1 MHz) (inset of Fig. 2) and tan δ_{max} increased (from 0.067 at 1 kHz to 0.098 at 1 MHz) (inset of Fig. 2) upon increasing frequency. One can therefore see that lowering the percentage of added PT in PMZT caused a downward shift by 28 ºC in T_m, and caused ε_{max} to increase by 2014 with a decrease in dielectric loss [4].

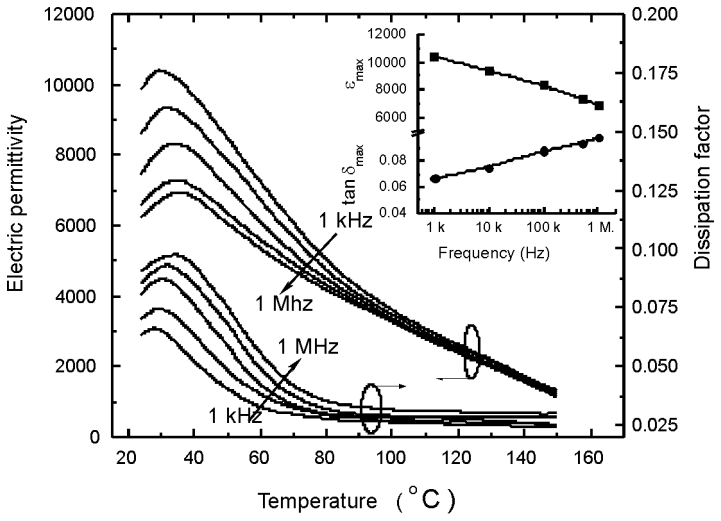

Fig. 2. Temperature dependence of electric permittivity of $0.90Pb[(Mg_{2/3}Zn_{1/3})_{1/3}Ta_{2/3}]O_3$–$0.10PbTiO_3$ at 1 kHz, 10 kHz, 100 kHz, 500 kHz and 1 MHz. The inset shows the variation of maximum value of ε and tanδ upon frequency

The results obtained in PMZT-PT(90/10) thus makes it a potential candidate for applications in devices. The sharp decrease in the electric permittivity as a function of increasing frequency can be explained in terms of the interfacial polarization. Contribution from interfacial polarizability comes due to the presence of two layers of materials of different conductivity. Here the motion of the charge carrier occurs readily in the higher conductivity phase, but is interrupted at the phase boundary due to the lower conductivity of the second phase [7]. In the case of polycrystalline ceramics, this is commonly observed if the grains are semiconducting and the grain boundaries are insulating. The semiconductive grains in PMZT-PT ceramics are believed to be caused by oxygen loss during firing at higher temperatures, in accordance with the reaction [8]:

$$O_0 \longleftrightarrow \frac{1}{2}O_2 \uparrow + V_0^{\bullet\bullet} + 2e^-$$

where all the species conform to the Kröger–Vink defect notation. These defects affect impedance and capacitance in the formation of barrier layers at the grain–grain boundary interface. During cooling after sintering, the reverse reaction occurs, but, due to the insufficient time available during cooling, reoxidation takes place and is restricted only to grain boundaries. This results in a difference between the resistance of grain boundary and grain, giving rise to a barrier [9]. The build-up of charges at the grain –grain boundary interface causes large polarization, resulting in a high electric permittivity at lower frequencies. Also, analogous to many other dipolar glassy systems, PMZT-PT(90/10) ceramic exhibits pronounced dispersion peaks in $\tan\delta$ (Fig. 2), which shift to lower temperatures (from 33 °C at 1 MHz to 27 °C at 1 kHz) as frequency decreases.

In order to examine the diffuse phase transition and relaxor more closely, the relationship between ε and T above T_m can be expressed by the modified Curie–Weiss law [10]:

$$\frac{1}{\varepsilon} - \frac{1}{\varepsilon_m} = \frac{(T - T_m)^\gamma}{C'} \tag{2}$$

where $C' = 2\varepsilon_m\delta^\gamma$ is the modified Curie–Weiss constant, δ is the diffusivity parameter, and γ is the diffuseness exponent, which can vary from 1, for normal ferroelectrics, to 2 for relaxor ferroelectrics. Equation (2) can be solved graphically using a log-log plot, as shown in Fig. 3. The slope of the curve represents the value of the critical exponent, while the intercept gives the diffuseness parameter according to the following equation:

$$\delta = \left(\frac{e^{-\text{intercept}}}{2\varepsilon_m}\right)^{1/\gamma} \tag{3}$$

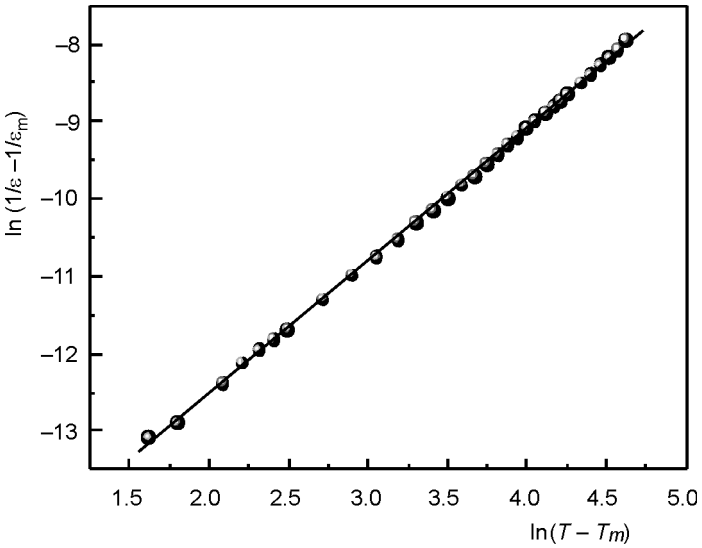

Fig. 3. Dependence of $\ln(1/\varepsilon - 1/\varepsilon_m)$ on $\ln(T - T_m)$ for $0.90Pb[(Mg_{2/3}Zn_{1/3})_{1/3}Ta_{2/3}]O_3$–$0.10PbTiO_3$ at 1 kHz

Linear regression analysis established $\gamma = 1.71$, $\delta = 32.36$ and $C' = 79.01\times10^5$ °C at 1 kHz which clearly indicates the DPT, and is found to increase with increase in frequency. It is expected that some disorder in the cation distribution (compositional fluctuations) causes the DPT where the local Curie points of different microregions are statistically distributed around the mean Curie temperature [11]. The non-equality of phase transition temperature obtained from ε–T and tan δ–T measurement also confirms the DPT.

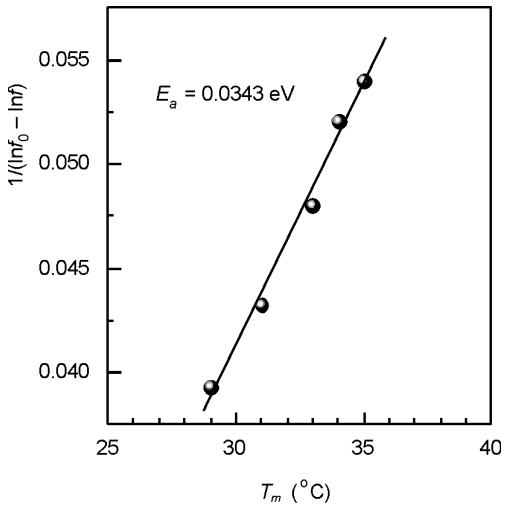

Fig. 4. Verification of the Vogel–Fulcher equation

Figure 4 shows the variation of $1/(\ln f_0 - \ln f)$ against the inverse of temperature T_m. Solid circles represent the experimental data. A linear least-squares fit of dielectric data, as in Eq. (1), calculates the values of E_a, f_0 and T_f as 0.0343 eV, 1.104×10^{14} Hz and 13.54 ºC, respectively. These values are also consistent with earlier reports on similar systems [4, 12–17]. The value of f_0 is found to lie in the optical frequency range of lattice vibrations. An excellent fit of the Vogel–Fulcher law with the experimental data constitutes strong evidence for a static freezing temperature of thermally activated polarization fluctuations in PMZT-PT. Therefore, dielectric relaxation in PMZT-PT may be considered as analogous to the magnetic relaxation in spin-glass system with polarization fluctuations above a static freezing temperature.

The polydispersive nature of dielectric relaxation can be checked through the Cole–Cole plots [18]. For pure monodispersive Debye relaxation, one expects semicircular plots, with the centre located on the ε' axis. However, for polydispersive relaxation, these Argand plane plots are close to circular arcs with end-points on the real axis, and with the centre lying below this axis. The complex electric permittivity is known to be described by the empirical relation:

$$\varepsilon^*(\omega) = \varepsilon' - i\varepsilon'' = \varepsilon_\infty + \frac{\Delta\varepsilon}{1+(i\omega\tau)^{1-\alpha}} \tag{4}$$

where $\Delta\varepsilon = \varepsilon_s - \varepsilon_\infty$ is the contribution of the relaxator to static permittivity ε_s, ε_∞ is the contribution of higher frequency polarization mechanism, τ (= $1/2\pi f$) is the mean relaxation time of the relaxators. The parameter characterizes the distribution of relaxation times, and it increases as the number of internal degrees of freedom of relaxators becomes larger.

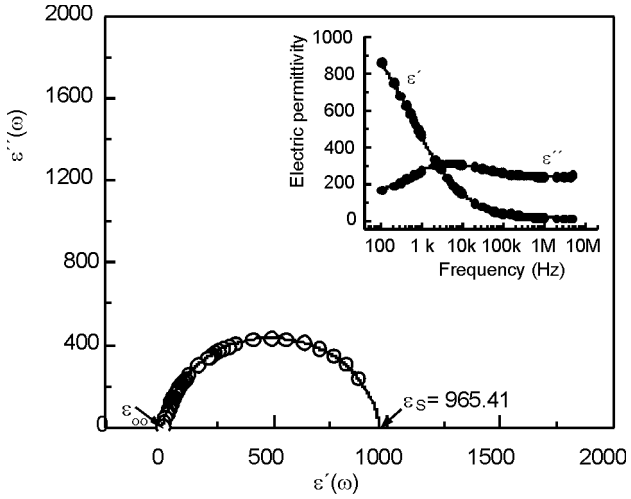

Fig. 5. Cole–Cole diagram for 0.90Pb[$(Mg_{2/3}Zn_{1/3})_{1/3}Ta_{2/3}$]$O_3$–0.10$PbTiO_3$ at 350 °C. The inset shows the variation of real and imaginary parts of ε with frequency at 350 °C

The parameter α provides a measure of departure from an ideal Debye condition. It can, however, be determined from the location of the centre of the Cole –Cole circles: Figure 5 depicts a representative plot for PMZT-PT at 350 ºC. When α tends to zero (i.e., $(1 - \alpha) \rightarrow 1$), Eq. (4) reduces to a classical Debye's formalism. It can be inferred from this plot that the relaxation process is of polydispersive non-Debye type ($\alpha \cong 0.011$). The parameter α was determined from the angle subtended by the radius of the circle with the ε' axis passing through the origin of the ε'' axis. The value of $\Delta\varepsilon$ is estimated to be 961. Also, as can be seen from the inset in Fig. 5, the value of ε' decreases as frequency increases, while ε'' shows a peak at 3 kHz. The value of τ comes to be 5.305×10^{-5} s.

3.3. Impedance studies

The inset in Figure 6 shows the real and imaginary parts, Z' and Z'' respectively, of impedance variation at frequencies corresponding to the temperatures 300 ºC, 325 ºC and 350 ºC. It can be seen that the magnitude of Z' decreases as a function of increasing frequency and increasing temperature. The Z' values for all temperatures converge above 100 kHz. This may be attributable to the release of space charges. The curves

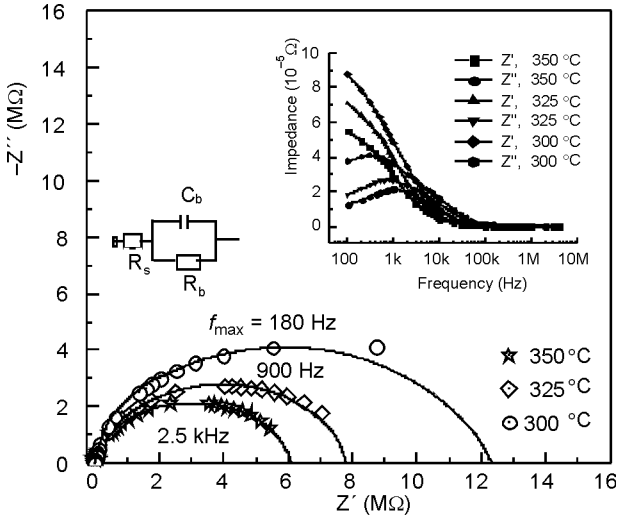

Fig. 6. Complex impedance of $0.90Pb[(Mg_{2/3}Zn_{1/3})_{1/3}Ta_{2/3}]O_3$–$0.10PbTiO_3$ at various temperatures. The inset shows dependence of Z' and Z'' on frequency at 300 °C, 325 °C and 350 °C

also display a single relaxation process, indicating an increase in a.c. conductivity upon increasing temperature and frequency. From the profile of the curves it can be inferred that the complex impedance of the electrode/ceramic/electrode capacitor is the sum of the single RC-circuit (Debye relaxators) in a parallel combination. Therefore,

$$Z^*(\omega,T) = Z_o(T)\int_0^\infty \frac{g(\tau,T)d\tau}{1+i\omega\tau} \tag{5}$$

which gives

$$Z'(\omega,T) = Z_o(T)\int_0^\infty \frac{g(\tau,T)d\tau}{1+\omega^2\tau^2} \tag{6}$$

$$Z''(\omega,T) = Z_o(T)\int_0^\infty \frac{\omega T\ g(\tau,T)d\tau}{1+\omega^2\tau^2} \tag{7}$$

where $\tau = RC$ is the relaxation time, $g(\tau,T)$ is the distribution function: this determines the distribution of relaxation times. In the case of a broad spectrum, i.e. $\tau_{min} \le \tau \le \tau_{max}$, Z'' can be approximated as (see [19])

$$Z'' \cong KZ_0(T)g(\tau,T) \tag{8}$$

where K is a constant. Therefore, $Z''(\omega,T)$ should provide the information about the distribution function $g(\tau,T)$. The curve for Z'' vs. frequency shows that the Z'' values reach a maximum (Z''_{max}) which shifts to higher frequencies as temperature increases. This also indicates a single relaxation process in the system. The variation profile of Z' and Z'' vs. frequency resembles the variation of ε' and ε'' vs. frequency (Fig. 5, inset). Figure 6 shows the plot of Z' vs. Z'' for PMZT-PT ceramic at three different temperatures. A semicircle could be traced from 300 °C onwards. All these curves start almost at the origin ($R_\infty \sim 20\ \Omega$) and hence there should be a series resistance (R_s) of 20 Ω for the LCR circuit representation of the sample. The high frequency semicircle may be ascribed to the parallel combination of bulk resistance (R_b) and capacitance (C_b) of PMZT-PT. The appropriate equivalent circuit comprising of R_s, R_b and C_b is shown in the inset in Fig. 6. The value of R_b can be directly obtained from the intercept on the Z' axis, the frequency at which the inflection point occurs in Z'' yields the measure of the relaxation time (τ_b), since at this point $\omega\tau_b = 1$ and the value of C_b can be calculated using the relation:

$$2\pi f_{max} R_b C_b = 1 \tag{9}$$

where f_{max} is the frequency at the maximum of the semicircle. It is observed that the peak maxima of the plots decrease, and f_{max} shifts to higher values when temperature increases. Furthermore, the values for R_b, C_b and τ_b decrease as temperature increases (Table 1). The decrease in the value of R_b upon increasing temperature reveals a negative temperature coefficient of resistance (NTCR) in PMZT-PT. It can also be noticed that the complex impedance plots are not represented by full semicircles; rather, the semicircular arcs are depressed and the centres of the arcs lie below the real (Z') axis, similarly to the Cole–Cole plot (Fig. 5). The complex impedance in such situations has been described by the Cole–Cole formalism [20]:

$$Z^*(\omega) = Z' + iZ'' = \frac{R}{1 + \left(\frac{i\omega}{\omega_0}\right)^{1-n}} \tag{10}$$

where n represents a measure of how much the electrical response deviates from an ideal condition (i.e., $(1 - n) \rightarrow 1$ in Eq. (10) gives rise to a classical Debye formalism).

Table 1. Parameters obtained from the complex impedance plots at various temperatures

Parameter	Temperature [°C]		
	300	325	350
R_b [Ω]×10^{-5}	12.425	7.808	6.104
C_b [F]×10^{10}	7.113	2.264	1.043
τ_b [s]×10^4	8.842	1.768	0.637
n	0.033	0.022	0.011

Fitting the complex impedance data to Eq. (10) gives a non-zero value of n which decreases when temperature rises (Table 1), and hence confirms the polydispersive nature of dielectric relaxation in PMZT-PT. This may be due to the presence of distributed elements in the material–electrode system [18]. It is also noticed that as temperature increases $n \rightarrow 0$, following the classical Debye type relaxation. At 350 ºC, an almost full semicircle is observed ($n = 0.011$). Therefore, one can deduce that with the temperature increasing, the complex impedance data approaches the Debye type relaxation.

Hence, the relaxor ferroelectrics at high temperature could be considered as an ensemble of uncorrelated Debye-like relaxators with some relaxation times. As the temperature is lowered, the correlation among the Debye relaxators becomes stronger through the formation of nanopolar clusters [19]. Since the relaxation times of the relaxators within polar clusters are distributed over a wide spectrum at lower temperatures, their response to external fields are in a different time domain. This results in the deviation from the Cole–Cole plot with partial semicircular arcs. It is clear from Fig. 6 that as the measuring temperature decreases, the centre of the Cole–Cole semicircles shifts below the Z' axis, inferring a possible average profile of various Cole–Cole semicircles. This cannot arise due to any other secondary factor such as interfacial capacitance or defects whose relaxation times are assumed to be superimposed with the actual ceramic response. If we assume that the interfacial capacitance also exhibits a similar type of dielectric dispersion, the high temperature in the Cole–Cole plots would have been split into two discrete semicircles, not observed in the present case. The value of R^2 (regression coefficient) for all the data fits, quoted in this paper, is ≥ 0.9992.

4. Conclusion

Polycrystalline samples of PMZT-PT having cubic structure were prepared by the coulombite precursor method. The compound showed a relaxor behaviour with a diffuse phase transition. A high value (> 10 000) for the electric permittivity was obtained at 1 kHz, with the temperature of maximum permittivity near room temperature. Modelling the dielectric data using the Vogel–Fulcher law constitutes strong evidence for a static freezing temperature of thermally activated polarization fluctuations in PMZT-PT. Therefore, dielectric relaxation in PMZT-PT may be considered as analogous to the magnetic relaxation in spin-glass systems having polarization fluctuations above a static freezing temperature. Cole-Cole analysis indicated the relaxation to be of non-Debye type and the relaxation frequency shifting to the higher side with an increase in temperature. The deviation from a Debye profile in the present system may be attributed to the formation of the nanopolar clusters.

Acknowledgement

The authors (SNC and KP) acknowledge the financial support of the Department of Science and Technology (DST), New Delhi (Ref. No.: SP/S2/M-15/97).

References

[1] BOKOV V.A., MYL'NIKOVA I.E., Sov. Phys. Tech. Phys., 2 (1961), 2428.
[2] CHOI S.W., JUNG J.M., J. Kor. Phys. Soc., 29 (1996), S672.
[3] LEE S.H., JUNG J.M., CHOI S.W., J. Korean Phys. Soc., 32 (1998), S1013.
[4] PRASAD S., PRASAD K., CHOUDHARY S.N., SINHA T.P., Physica B: Cond. Matter, 364 (2005), 206.
[5] VOGEL H., Z. Phys., 22 (1921), 645.
[6] FULCHER G., J. Am. Ceram. Soc., 8 (1925), 339.
[7] SINGH S.P., SINGH A.K., PANDEY D., J. Mater. Res., 18 (2003), 2677.
[8] LEE S.B., LEE K.H., KIM H., Jpn. J. Appl. Phys., 41 (2002), 5266.
[9] CHEN D.R., GUO Y.Y., Electron. Element. Mater., 1 (1982), 25.
[10] UCHINO K., NOMURA S., Ferroelectr. Lett., 44 (1982), 55.
[11] PRASAD K., Ind. J. Eng. Mater Sci., 7 (2000), 446.
[12] VIEHLAND D., LI J.F., JANG S.J., CROSS L.E., WUTTING M., Phys. Rev. B, 46 (1992), 8013.
[13] TAGANTSEV A.K., Phys. Rev. Lett., 72 (1994), 1100.
[14] VIEHLAND D., JANG S.J., CROSS L.E., WUTTING M., J. Appl. Phys., 68 (1990), 2916.
[15] BOKOV A.A., LESHCHENKO M.A., MALITSKAYA M.A., RAEVSKI I.P., J. Phys: Cond. Matter., 11 (1999), 4899.
[16] KUMAR A., PRASAD K., CHOUDHARY S.N., CHOUDHARY R.N.P., Matter. Lett., 58 (2004), 3395.
[17] TU CHI-SHUN, CHAO F.-C., YEH C.-H., TSAI C.-L., Phys. Rev. B, 60 (1999), 6348.
[18] MACDONALD J.R., *Impedance Spectroscopy Emphasizing Solid Materials and Systems*, Wiley, New York, 1987.
[19] BONNEAU P., GARNIER O., CALVARIN G., HUSSON E., GAVARRI J.R., HEWAT A.W., MORREL A., J. Solid State Chem., 91 (1991), 350.
[20] COLE K.S., COLE R.H., J. Chem. Phys., 9 (1941), 341.

Received 6 September 2006
Revised 7 June 2007